REVIEW

EDUCATIONAL SERIES IN CONGENITAL HEART DISEASE

Cardiovascular MRI and CT in congenital heart disease

Kuberan Pushparajah BMBS BMedSci MD[1,2], Phuoc Duong MBChB MRCPCH[1,2], Sujeev Mathur MBBS[2] and Sonya V Babu-Narayan MBBS BSc PhD FRCP[3,4]

[1]School of Biomedical Engineering and Imaging Sciences, King's College London, London, UK
[2]Evelina London Children's Hospital, London, UK
[3]Royal Brompton Hospital, London, UK
[4]National Heart & Lung Institute, Imperial College London, London, UK

Correspondence should be addressed to K Pushparajah: kuberan.pushparajah@kcl.ac.uk

Abstract

Cardiac MRI and CT are increasingly used in the diagnosis and management of patients with congenital heart disease as an imaging adjunct to echocardiography. The benefits and limitations of both modalities are highlighted, with a focus on the anatomical, functional and haemodynamic information that can be gained from the different modalities. Deciding on the imaging modality of choice must also take into account patient factors such as age, compliance, the type of congenital heart disease, and previous procedures. Future developments in CT and MRI are also discussed.

Key Words

- congenital heart disease
- CMR
- cardiac magnetic resonance imaging
- cardiac CT
- paediatric cardiology

Introduction

Comprehensive imaging assessment of cardiac anatomy and physiology is a key component in the management of patients with congenital heart disease. Although echocardiography remains the primary imaging modality in this area, there is an established role for cardiovascular MRI (CMR) and computed tomography (CT) as an adjunct in the assessment of congenital heart disease (CHD). The role of multimodality imaging is increasingly being recognised, as outlined in several international position documents on the management of patients with congenital heart disease (1, 2, 3, 4). Each imaging modality has inherent advantages and limitations as summarised in Table 1.

The common advantage of CMR and CT is the ability to produce whole heart imaging, detailed visualisation of the extracardiac vasculature and its relationship to surrounding structures. Although fluoroscopic contrast-enhanced angiography by means of invasive cardiac catheterisation is a reliable and long-established means of demonstrating cardiac anatomy, CMR and CT have the advantage of being non-invasive. Contrast-enhanced cardiac CT is fast and is able to delineate very small structures such as coronary arteries very well due to its high spatial resolution. CMR although more time consuming, has the advantage of being free of radiation, while also able to provide important information on cardiac function, tissue characterisation and circulatory haemodynamics by means of accurate and reproducible measurements of ventricular volumes and flows within vessels. Deciding on the imaging modality of choice is based on the clinical question, patient factors and availability of the diagnostic tools required. Due to the scope of the subject, the focus of this review is predominantly on its use in children.

https://erp.bioscientifica.com
https://doi.org/10.1530/ERP-19-0048

Table 1 Characteristics of different imaging modalities.

	2D echo	3D echo	Cardiac catheterisation	CT	CMR
Radiation	–	–	++	+(+)	–
Temporal resolution	<5 ms	20–200 ms	1–10 ms	50–135 ms	20–50 ms
Spatial resolution	0.5–2.0 mm		0.3–1.2 mm	0.5 mm	0.8–2.0 mm
Quantitative ventricular function	++	++	+	++	+++
Ventricular volumetric	+	++	–	+	+++
Flow in vessels	+	–	+	–	+++
3D whole heart imaging	–	++	++	+++	+++
Atrioventricular valve assessment	++	+++	+	+	++
Semilunar valve assessment	++	+++	+	++	+++
Myocardial tissue characterisation	++	+	+	+	+++
Pressure measurements/estimation	+++	–	+++	–	++

Cardiovascular MRI

CMR has the advantage over other forms of imaging in that it is free of radiation, is able to interrogate the heart in any geometry, and provides highly accurate and reproducible assessment of ventricular volumes and flows (5). It is considered the gold standard for imaging in the assessment of ventricular volumes and flows and there are clear guidelines for the use of CMR in the assessment of CHD (6, 7). It is particularly useful as patients with CHD often require repeat imaging as part of longitudinal surveillance of a life-long condition (8). The main limitations are where patients have significant metallic artefact impairing imaging of the heart, or claustrophobia precluding a detailed cardiac assessment.

How an MRI image is formed

MRI exploits the fact that our bodies are largely made up of water, and each hydrogen atom in a water molecule has a proton and electron, with the proton rotating around its own axis (9). The hydrogen atom is exploited by MRI, as the nuclei of hydrogen atoms are randomly orientated with a net magnetisation of zero outside a magnetic field. The nuclei align in the direction of a strong magnetic field (B0) when a patient is placed inside the bore of an MRI scanner. There are varying field strengths of the magnets, but these are mainly 1.5–3T in CMR. This produces a net magnetisation (M) parallel to the scanner bore which is then manipulated by an external radiofrequency (RF) pulse to generate images. During relaxation following the RF pulse, the protons release their excess energy, partly as RF waves which are captured by an RF receiver coil in order to produce an image. The MRI image is reconstructed using an algorithm, known as 2D Fourier transform. The MRI signals are digitally sampled and stored as data points in a domain known as k-space. The information stored in k-space is related to the image via the Fourier transform, forming the basis of the image reconstruction process.

Practical considerations in CMR

CMR studies require a patient to lie still within the magnet bore for the duration of the study. Therefore, infants, small children and older patients who are unable to comply have traditionally required sedation or general anaesthesia. Some of the common sequences used in CMR also perform better with patient breath-holds which can be challenging for some. Acquisition of images can be quite noisy, and patients are given headphones both for ear protection and in order to hear the operator including when reassurance, explanation or breathing instructions are being given. However, with appropriate preparation, most patients are able to comply. There are newer, accelerated CMR sequences which allow for quicker scan times of a few seconds without the need for breath-holds. These are not only more acceptable to the patient but may replace the need for general anaesthesia or sedation in younger patients.

The major consideration is that of MRI safety, and both patients and staff have to be screened appropriately by trained radiology staff before approaching the magnet. All institutions will have an MRI safety policy which will have to be adhered to.

CMR assessment of anatomy

2D imaging

It is possible to interrogate the heart in any desired plane with MRI, hence dynamic 2D cine CMR imaging of the heart allows both anatomical and functional assessment of the heart. Unlike echocardiography, CMR is not limited by the

https://erp.bioscientifica.com
https://doi.org/10.1530/ERP-19-0048

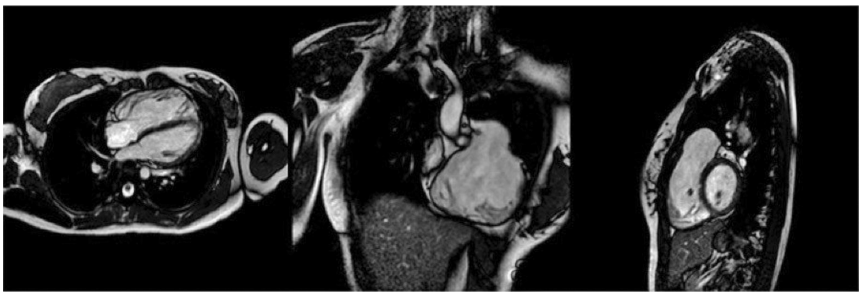

Figure 1
Balanced SSFP cine imaging in a patient with a dilated RVOT, pulmonary regurgitation and dilated RV post repair of tetralogy of Fallot (Video 1).

available acoustic windows. The workhorse in CMR for this is the balanced steady state free-precession (bSSFP) sequence, where the blood pool appears bright, with excellent contrast from the neighbouring myocardium which appears black, also known as 'bright-blood' sequences. These geometries are carefully planned by alignment to orthogonal planes to ensure images of interest are not foreshortened. This can be seen in Fig. 1 (Video 1) where a subjective assessment of the geometry, size, and function of the cardiac structures can be made from a series of cine images. Multiple 2D cine stacks across the whole chest in an axial, coronal or sagittal plane can also be helpful in the assessment of leaks or narrowing in complex intracardiac baffles such as the systemic and pulmonary venous baffles following the atrial switch procedure. However, they cannot be reconstructed into a rendered view as the acquisitions are not isotropic in all three imaging planes.

Video 1
Balanced SSFP video imaging in a patient with a dilated RVOT, pulmonary regurgitation and dilated RV post repair of tetralogy of Fallot. View Video 1 at http://movie-usa.glencoesoftware.com/video/10.1530/ERP-19-0048/video-1.

Static images of the heart by 'bright blood' and 'black blood' imaging can be obtained in a similar planning method to the 2D cine images described above. In 'black blood' images the blood-pool appears dark, particularly in areas with fast-flowing blood. This is because the specific CMR sequence results in the fast-flowing blood having no net magnetisation; hence, no signal as shown in Fig. 2.

3D imaging

3D whole heart imaging including images of the major blood vessels is key in the assessment of CHD as it allows for sequential segmental analysis of the cardiac connections and the great vessels. It can also be used to understand the complex spatial relationships of intracardiac structures to plan complex surgery or interventions.

Contrast-enhanced CMR angiography (MRA) is extremely useful to delineate the vascular structures which can be frequently abnormal in CHD. The image acquisition techniques are now accelerated which allows for multiple image acquisitions over time as the contrast passes through the circulation resulting in time-resolved 3D angiography (Fig. 3 and Video 2). While these provide excellent visualisation of the major vessels, branch pulmonary arteries and collateral vessels, these images are not ECG gated and are susceptible to cardiac motion; hence, structures such as coronary arteries are not well visualised. Additionally, the image acceleration methods compromise the spatial resolution which is lower than conventional contrast-enhanced CT images. Patients with renal dysfunction should be assessed carefully prior to the administration of gadolinium-based contrast, as those with an estimated glomerular filtration rate <30 mL/min/1.73 m^2 are considered at highest risk of nephrogenic systemic fibrosis (NSF), a rare and serious condition that involves fibrosis of primarily the skin and subcutaneous tissue. Given congenital heart disease patients may undergo many CMR scans over a lifetime there is interest to avoid contrast injection at every attendance and rather use this selectively where indicated in order to reduce lifetime cumulative dose, and potential concerns about long term brain deposits.

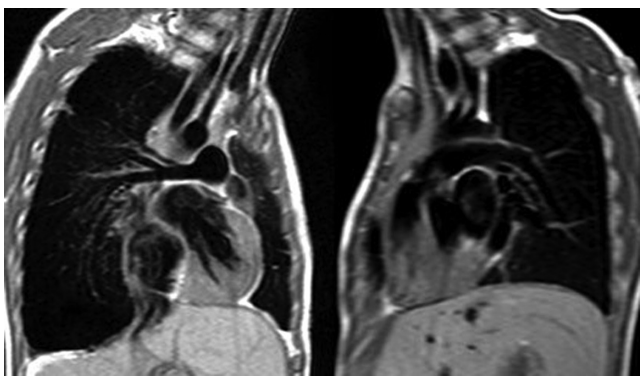

Figure 2
Two-dimensional black blood images of the right and left pulmonary arteries.

https://erp.bioscientifica.com
https://doi.org/10.1530/ERP-19-0048

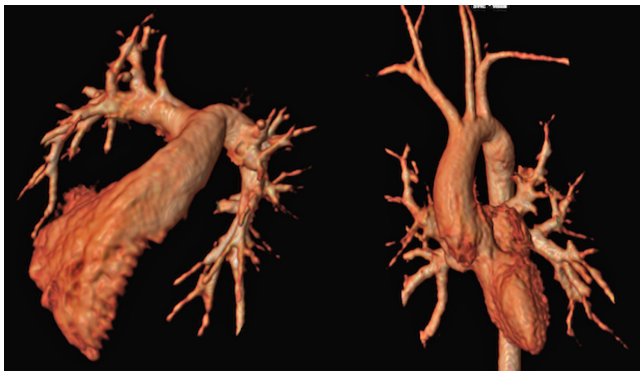

Figure 3
Contrast-enhanced MR angiography of the right ventricle and branch pulmonary arteries, and the pulmonary veins, left ventricle and aorta.

Video 2
Contrast-enhanced MR angiography of the right ventricle and branch pulmonary arteries, and the pulmonary veins, left ventricle and aorta. View Video 2 at http://movie-usa.glencoesoftware.com/video/10.1530/ERP-19-0048/video-2.

Non-contrast-enhanced 3D whole heart imaging is achieved by 3D balanced SSFP imaging, paired with ECG-gating and a respiratory navigator. The effect of respiratory motion is minimised by the use of a respiratory navigator set to only acquire images at end expiration, while cardiac motion is addressed by only acquiring images during the systolic and diastolic rest periods of the heart. This allows for high-quality, high spatial resolution images of the heart with excellent visualisation of the intracardiac anatomy and coronary artery anatomy compared to 3D MRA (Fig. 4A and Video 3). This remains the most used method of non-contrast 3D whole heart imaging in CHD. The 3D image can be interrogated on a multiplanar reformat platform to allow for accurate and reproducible measurements of cardiac structures (Fig. 4B). As vessel size is dynamic over the course of the cardiac cycle, it is crucial to record the phase of the cardiac cycle in which the image was obtained for the associated measurement and for the purposes of serial or intermodality comparison. An example of this is in sizing the right ventricular outflow tract in repaired tetralogy of Fallot for suitability for percutaneous pulmonary valve implantation. In the presence of pulmonary regurgitation, the main pulmonary artery is very expansile with significant differences in dimensions in systole and in diastole (10). Non-contrast-enhanced 3D imaging of this type is also very useful for the routine and serial surveillance of patients with inherited aortopathies and the various congenital heart lesions where aortic dilation is common or of concern to monitor rates of aortic dilation. 3D cross-sectional imaging of the aorta allows more certainty regarding perpendicularity to the vessel wall. This 3D whole heart imaging method

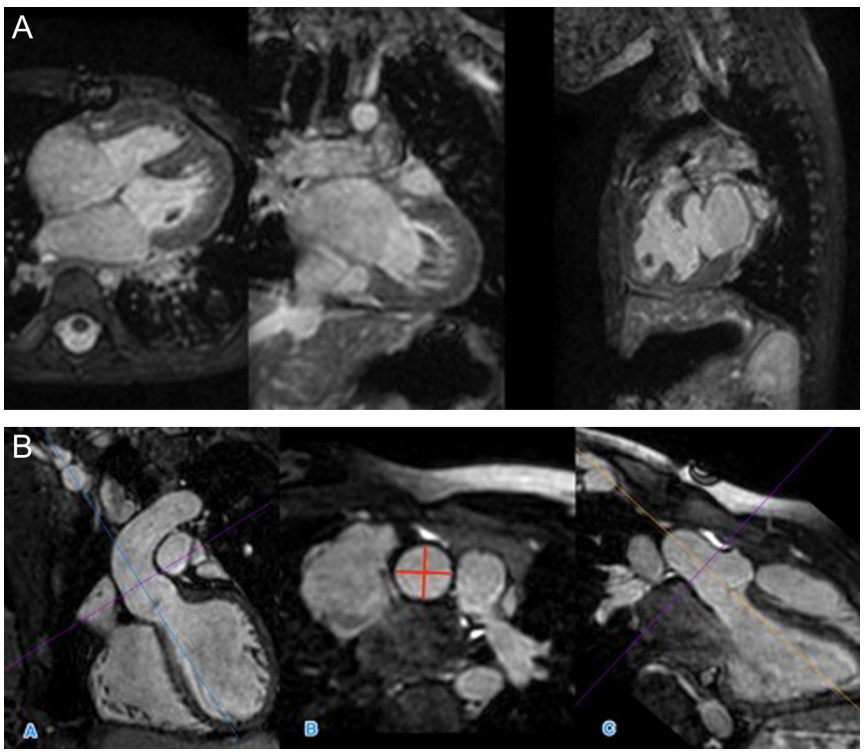

Figure 4
(A) 3D SSFP dataset, in coronal, axial and sagittal planes. (B) MPR of 3D SFFP image demonstrating measurement of the sinotubular junction of the aorta. This is measured in image B, from orthogonal planes (A and C).

https://erp.bioscientifica.com
https://doi.org/10.1530/ERP-19-0048

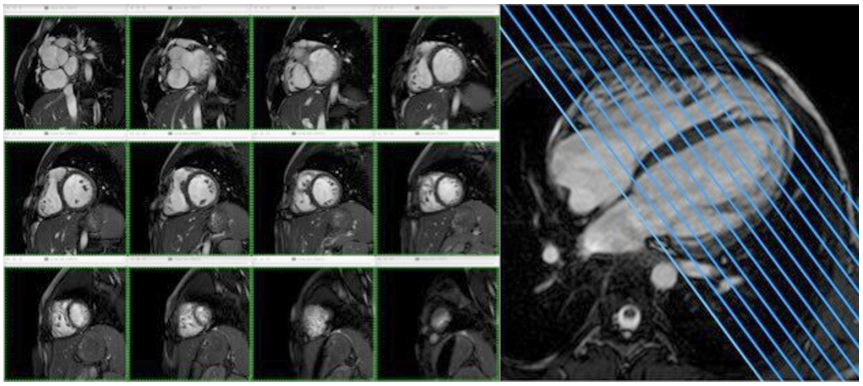

Figure 5
Ventricular volumes are generated from a stack of 2D cine CMR slices across the ventricle.

is however susceptible to motion artefact from turbulent flow within a vessel or chamber, and metallic artefact from stents or devices. In practice, a number of different sequences are used for clinical interpretation with regards sizing and suitability including appropriately orientated cine images where maximum and minimum diameters in systole and diastole are clear.

Video 3
3D SSFP dataset, in coronal, axial and sagittal planes.
View Video 3 at http://movie-usa.glencoesoftware.com/video/10.1530/ERP-19-0048/video-3.

Ventricular volumes, function and flow

CMR is considered the gold standard for the assessment of ventricular volumes, function and flows. Ventricular volumes are derived from manual or semi-automated segmentation of the endocardial borders of every slice of a 2D cine stack across the whole ventricle. Each slice is typically 6–10 mm thick, capturing 25–40 phases of the whole cardiac cycle. The ventricular stroke volume and ejection fraction is derived from the measured end systolic and end diastolic volumes of the ventricle (Fig. 5). The addition epicardial borders to the endocardial segmentation allows for calculation of ventricular mass (Table 2). Measuring ventricular volumes and function in this way is proven to have high inter-user and intra-user variability (5, 11).

Strain imaging

Conventional markers of function such as stroke volume and ejection fraction are not very sensitive and may only become abnormal in the late stages of ventricular failure. Echocardiographic assessment of strain is widely applied in the assessment of myocardial deformation to detect earlier changes but can be challenging due to the acoustic windows. CMR feature tracking (CMRFT) is now increasingly possible with feature tracking analysis tools which can be used on 2D cine images already acquired from a routine study. The features tracked on CMR are those of different signal intensity at the border between blood pool and myocardium, instead of the motion of individual pixels or group of pixels in echocardiography (Fig. 6). CMRFT is not limited by acoustic windows and has good spatial resolution; however, temporal resolution is reduced compared to echocardiography (12). Other myocardial deformation quantification methods by CMR are more established and are considered more the gold standard such as myocardial tagging or displacement encoding (DENSE) imaging, but these require the acquisition of extra images and time. There are already some data on the clinical value of CMRFT in CHD for prognostication in patients with tetralogy of fallot (13, 14).

Flow

Flow is measured by velocity encoded phase-contrast MRI. The signal amplitude and therefore the brightness of each voxel is proportional to the mean flow velocity within that voxel. The maximum velocity in one direction appears white, and then black in the opposite direction. There is a range of software available to quantify flow in vessel, by contouring the flow within a region of interest and generating a flow rate from the mean velocity and cross-sectional area as

Table 2 Summary of measured and calculated functional parameters by CMR.

Measured CMR parameters	Calculated parameters
EDV and ESV (mL)	SV = EDV – ESV (mL/beat)
Wall volume (mL)	EF = (SV/EDV) × 100 (%)
Heart rate (bpm)	CO = SV × HR (L/min)
	Mass = Wall volume × 1.05 (g)

CO, cardiac output; EDV, end diastolic volume; EF, ejection fraction; ESV, end systolic volume; SV, stroke volume.

https://erp.bioscientifica.com
https://doi.org/10.1530/ERP-19-0048

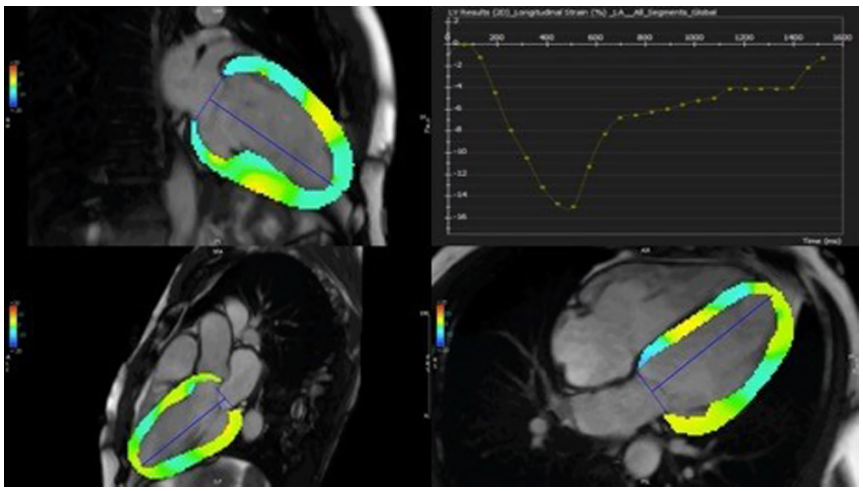

Figure 6
CMRFT quantifying global longitudinal strain of the left ventricle.

seen in Fig. 7. It is crucial that there is appropriate planning of the flow by aligning the sample acquisition at the true short axis of the vessel derived from two orthogonal images. Careful attention must also be paid to ensure the voxel size is appropriate for meaning sampling of blood flow velocities, with appropriate peak velocity limits selected to avoid issues of aliasing and undersampling (6).

In the presence of relatively laminar flow, CMR has been shown to be very reliable and reproducible. However, it is not always possible to measure flow in very turbulent, high velocity regions or in very small vessels. Therefore, some flows have to be calculated as shown in Fig. 8A. It has also been shown to be accurate for shunt quantifications in CHD (15). Atrioventricular valve regurgitant fraction is the difference in flow in the semilunar valves from the ventricular stroke volume of the corresponding chamber, expressed as a percentage of the ventricular stroke volume (e.g. mitral regurgitant fraction = (LV SV – Ao flow) ÷ LV SV). Aortopulmonary collateral vessels are often very small in Fontan patients but can be reliably calculated using flows from other parts of the circulation (16, 17) as shown in Fig. 8B).

Four-dimensional flow (4D flow)

Four-dimensional flow (4D flow) CMR is a technique involving phase-contrast CMR with flow encoded in all three spatial directions relative to all three dimensions of space and to the additional dimension of time along the cardiac cycle (3D + time = 4D). The spatial resolution is isotropic to 1.5–3 mm with a temporal resolution of about 30–40 ms. The sequence however has a long acquisition time of 5–25 min. It allows for the quantification of flow, visualisation of flow pathways within the heart and blood vessels, and estimation of the haemodynamic effects on the myocardium or vessel wall (18). It is best incorporated into a 3D whole heart image to allow for correlation of the flow pattern to a vessel or chamber of interest (Fig. 9 and Video 4). 4D flow may allow less operator-dependent flow acquisition and more opportunity for accurate offline measurements that can be determined according to findings after the study. This is especially relevant in congenital heart disease where multiple regurgitant or stenotic lesions and shunts may be present.

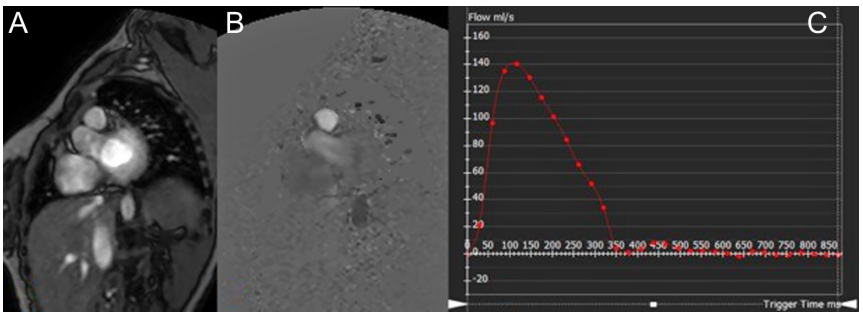

Figure 7
Magnitude (A) and phase-contrast flow images (B) and flow map measurement using MR analysis software (C) (in this case the main pulmonary artery). The flow value is the area under the curve.

https://erp.bioscientifica.com
https://doi.org/10.1530/ERP-19-0048

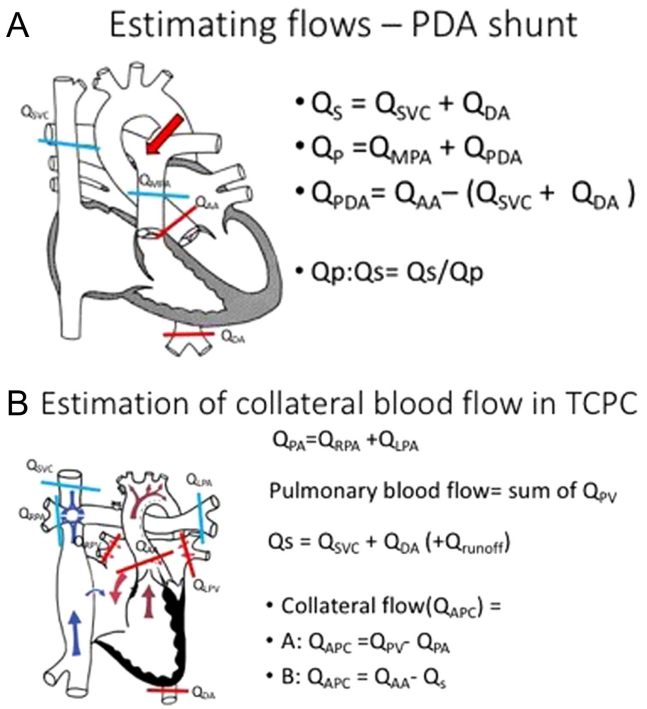

Figure 8
(A) Estimation of flow from a PDA. (B) Estimation of aortopulmonary Collateral flow in a Fontan.

Video 4
4D flow image of a patient with coarctation of aorta. View Video 4 at http://movie-usa.glencoesoftware.com/video/10.1530/ERP-19-0048/video-4.

Tissue characterisation

Myocardial fibrosis

Myocardial fibrosis is an important sequela of maladaptation from abnormal stresses on the heart or from ischemia. Reactive interstitial fibrosis is characterized by an increase in collagen synthesis with little or no loss of viable myocardium. Replacement fibrosis is considered a response to myocyte cell death, with subsequent increase in type I collagen deposition and expansion of the extracellular matrix (19). The site and extent of fibrosis can be detected using a technique whereby scans are performed following administration of gadolinium, termed late gadolinium enhancement (Figs 10 and 11). There is an increased signal in the images from gadolinium retained within the expanded extracellular matrix in the region of fibrosis. The detection of fibrosis can aid prediction of adverse outcomes in patients and help stratify the need for close monitoring

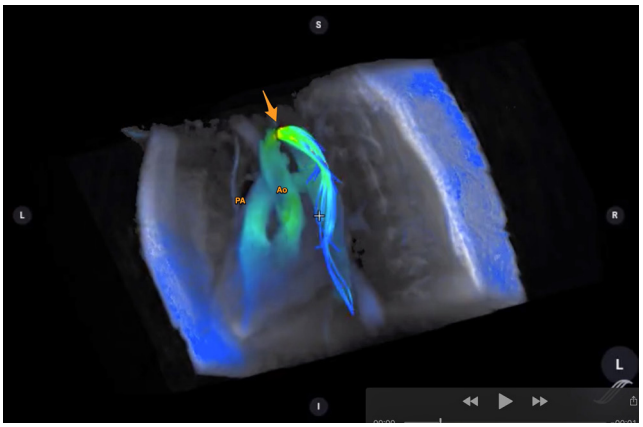

Figure 9
4D flow image of a patient with coarctation of aorta. The great vessels (pulmonary artery, PA and aorta, Ao) are annotated. The arrow points towards the coarctation. Flow acceleration is denoted in the flow velocity colour map as shown. (Image courtesy of Dr Francesca Raimondi, Hôpital Universitaire Necker – Enfants Malades, Paris, France.)

or intervention (20, 21, 22, 23). In CHD specifically, late gadolinium enhancement can be used to detect the extent of endocardial fibroelastosis which is poorly quantified on echocardiography.

Native T1 relaxation times increase with increased interstitial or replacement fibrosis. However, there are few published data on the prognostic value of native T1 in CHD as it is affected by several other diseases. ECV is the ratio of interstitial volume to the total myocardial volume. It is the most widely used imaging biomarker for interstitial fibrosis and is derived by comparing the native (precontrast) and postcontrast T1 times in the myocardium and in the blood pool and accounting for the hematocrit. However, there remains a limited place for this technique as a prognostic tool at present as T1 values vary according to the magnetic field strength, and there is a lack of vendor agnostic standards for both acquisition and postprocessing. In ischaemic heart disease, ECV is shown to predict mortality. To date, there are few data giving a compelling case as to how this can be usefully applied clinically in CHD which is a subject of active research.

CMR is also widely used for the evaluation of myocardial inflammation in acquired heart disease such as myocarditis (24, 25) but is outside the scope of this review on CHD. In brief, it is able to detect myocardial oedema by T2-weighted imaging, capillary leak and hyperaemia by early gadolinium enhancement and myocardial necrosis or fibrosis by LGE with associated changes in regional or global myocardial function (26).

https://erp.bioscientifica.com
https://doi.org/10.1530/ERP-19-0048

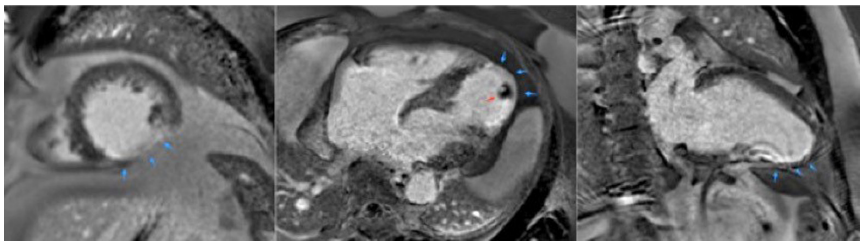

Figure 10
Late gadolinium enhancement images (LGE) of apical short axis, four-chamber and two-chamber view. LGE in the mid and apical inferior aspect of the LV. Infarcted area shows delayed gadolinium uptake (blue arrows pointing at the bright white structure). In this instance the effect is transmural. This corresponds to an invasive coronary angiogram finding of a thrombosed distal left anterior descending artery. The apical thrombus is also shown (red arrow).

Tumour characterisation

Cardiac tumours can be very challenging to define on echocardiography and CT. CMR with intravenous contrast not only helps define the size, location and extent of a cardiac tumour, but is able to characterise the tumour type based on the varying CMR signal characteristics and vascularity of different tissue types (27) (Fig. 12).

Bottom row: multiplanar reconstruction using 3D SSFP dataset to locate extent of the tumour within the heart.

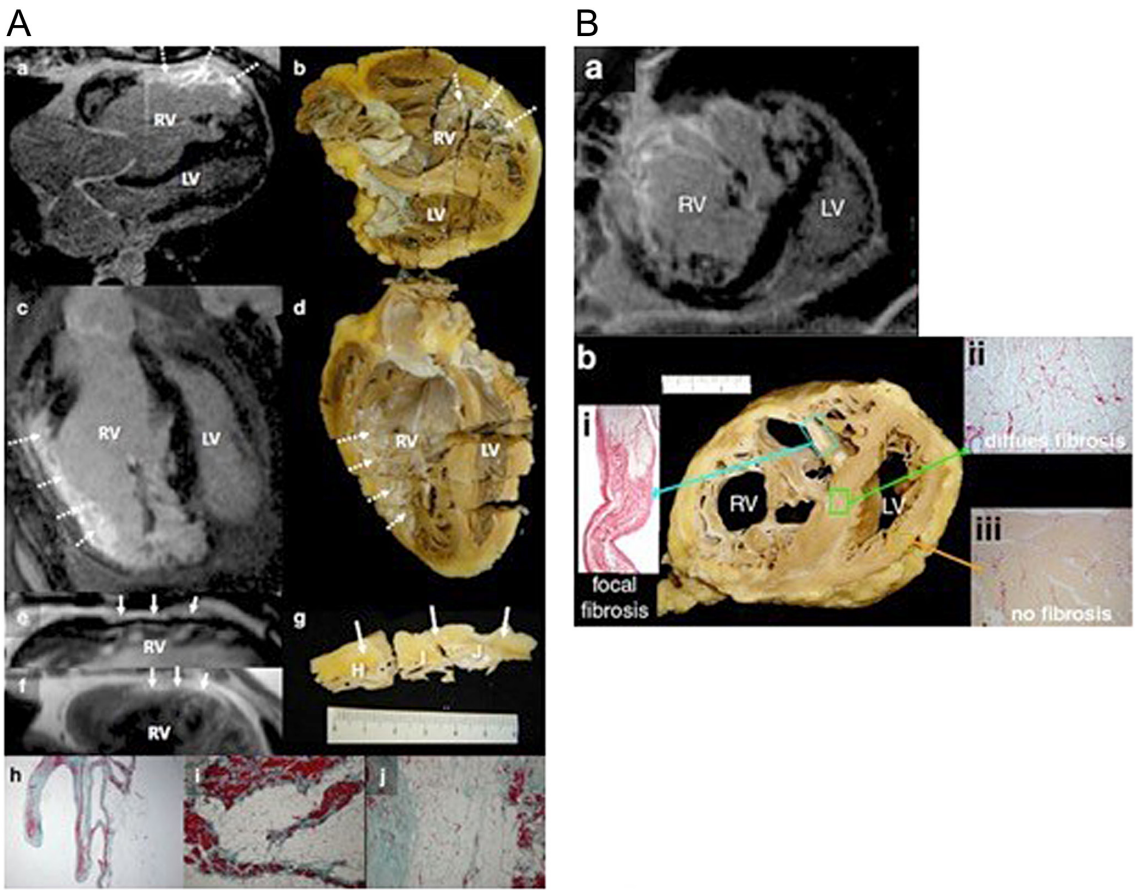

Figure 11
Macroscopic fibrosis and correlation with *in vivo* late gadolinium enhancement (LGE) cardiovascular magnetic resonance (CMR) in heart explanted during follow-up. LGE CMR (A and C) and corresponding photographs of macroscopic sections (B and D) showing excellent correlation of CMR LGE with visually fibrotic areas (arrows). The increased signal on balanced steady state free precession (E) and turbo spin echo (F; continuous arrows) is compatible with fat. In (G), the corresponding macroscopic specimen shows epicardial fatty infiltration (continuous arrows) but also right ventricular (RV) endocardial fibrosis. Corresponding histology is shown after staining with Masson's Trichrome; region (H) shows extensive replacement of the compact myocardium by fatty tissue, whereas the trabeculations lining the cavity contain myocardium (red) and extensive fibrous tissue (green, ×16). Regions (I) and (J) show extensive fatty and fibrous replacement (×100). (B) Microscopic fibrosis and correlation with *in vivo* LGE CMR. Extensive RV LGE (A; short axis CMR plane) corresponded with macroscopic fibrosis in the explanted heart (B; transverse specimen) with Picrosirius Red staining confirmed collagen in the area of macroscopic fibrosis and corresponding LGE (i inset). Apparently normal looking myocardium at ×25 magnification (ii) shows a lower degree of interstitial/diffuse fibrosis undetected by LGE CMR. No fibrosis was detected in the subpulmonary LV (iii) (22).

https://erp.bioscientifica.com
https://doi.org/10.1530/ERP-19-0048

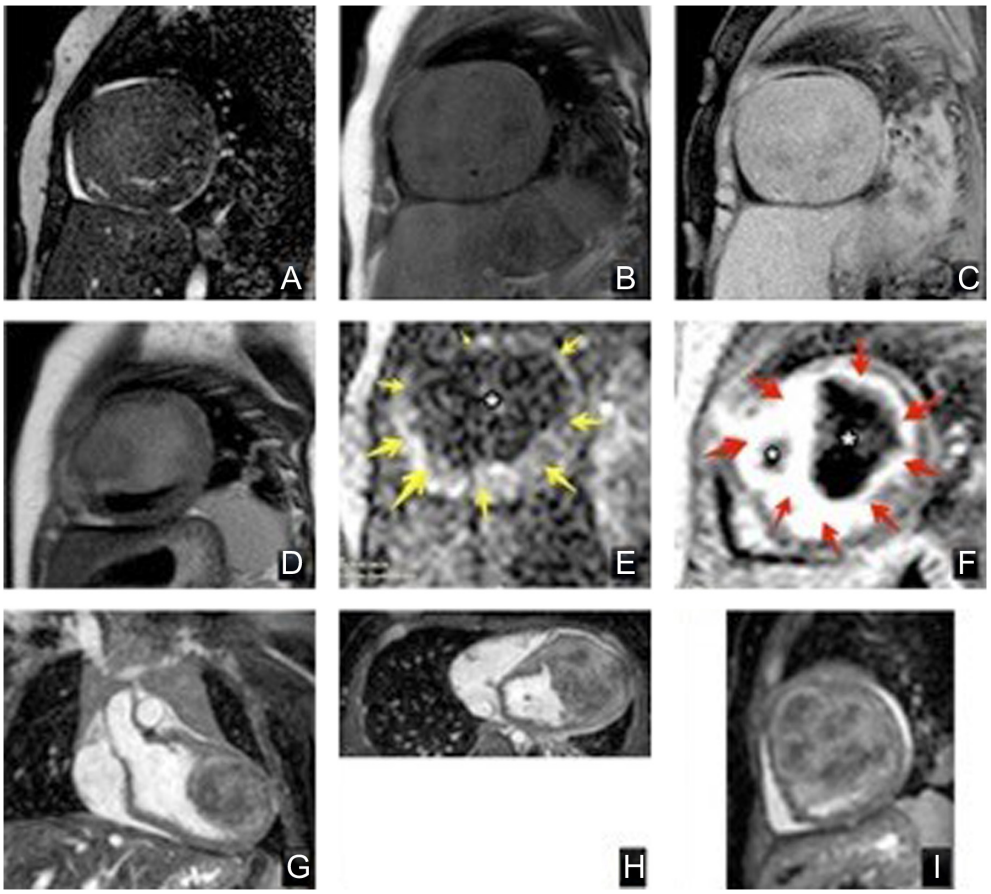

Figure 12
Tumour characterisation using different MR techniques, of a cardiac fibroma. Top row: (A) 2D balanced SSFP cine iso-intense signal with the myocardium, (B) T1 black blood with no fat suppression showing heterogenous texture with hyper-intense signal of the tumour capsule compared to myocardium and skeletal muscle, and (C) T1 black blood with fat suppression suggests that the tumour is not comprised of fatty tissue. Middle row: (D) T2 turbo-spin-echo black blood, (E) first pass perfusion image with no enhancement of the tumour (dark, *) compared to normal myocardium (yellow arrows) suggesting a non-vascular nature, and (F), late gadolinium enhancement, with high signal (red arrows) with a low signal dark core (*). Bottom row: multiplanar reconstruction using 3D SSFP dataset to locate extent of the tumour within the heart. Coronal (G), axial (H) and sagittal (I) view of the heart with location of the cardiac tumour.

Coronal (G), axial (H) and sagittal (I) view of the heart with location of the cardiac tumour.

Myocardial stress perfusion

The administration of a coronary artery vasodilator such as adenosine leads to increased myocardial perfusion, not matched in regions of impaired coronary perfusion. Administration of a gadolinium-based contrast agent allows these regions of hypoperfusion to be detected as dark areas during the study as seen in Fig. 13 (Video 5). This investigation can be applied to CHD patients with known coronary artery abnormalities, previous coronary interventions such as coronary artery transfer for the arterial switch procedure in transposition of the great arteries (28) or in acquired diseased affecting the coronary artery such as Kawasaki disease.

Video 5
Patient with transposition of great arteries post arterial switch operation and retro-pulmonary left coronary artery, presented with chest pain on exertion. Normal systolic function at rest. However, on stress perfusion, the images reveal perfusion defects in the left anterior descending artery and circumflex territories. View Video 5 at http://movie-usa.glencoesoftware.com/video/10.1530/ERP-19-0048/video-5.

Cardiac stents and devices: non-electronic

Most contemporary cardiac stents and occlusion devices are MRI conditional and safe to scan at 1.5 Tesla, with different profiles at higher filed strength magnets. It is important to note the exact device and assess the suitability to scan based on local safety policies. A list of

https://erp.bioscientifica.com
https://doi.org/10.1530/ERP-19-0048

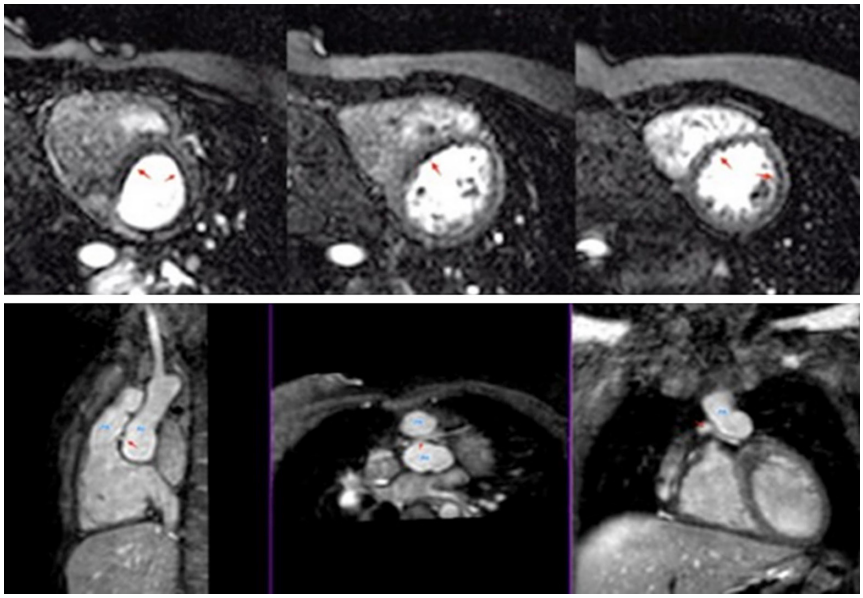

Figure 13
Patient with transposition of great arteries post arterial switch operation and retro-pulmonary left coronary artery, presented with chest pain on exertion. Normal systolic function at rest. However, on stress perfusion, the images reveal perfusion defects in the left anterior descending artery and circumflex territories. Lower row images show relationship between the pulmonary artery (PA), aorta (Ao) and left main coronary artery (red arrow) (Video 5).

these can be looked up on various databases (e.g. http://www.mrisafety.com/TMDL_list.php) or from the device manufacturer. Even if they are safe, there should be special consideration for the image sequences used to reduce the effects of image artefact (Fig. 14).

Cardiac implantable electronic devices

The presence of a pacemaker or implantable cardioverter defibrillator has traditionally been a contraindication for MRI. In recent years, there is increasing evidence that concern for serious adverse events are overstated, with large studies showing limited and manageable side effects (29). Newer MR conditional devices are now commonly available and are increasingly being implanted opening up the options for MRI scanning in this group. However, there are efforts to ensure that patients with older MR nonconditional devices are no longer denied non-cardiac MRI scans. MRI protocols with appropriate safety precautions and support are being put in place for this. There still remains variation in availability and practice. Although they may be safe to scan, they can still generate image artefacts which diminish the value of the CMR in some cases (Fig. 15) and protocols optimised for patients with devices *in situ* and experience in applying them is needed.

New developments in CMR

Fetal CMR

Fetal CMR has always been challenged by the lack of ECG gating of the fetal heart, the small size of the

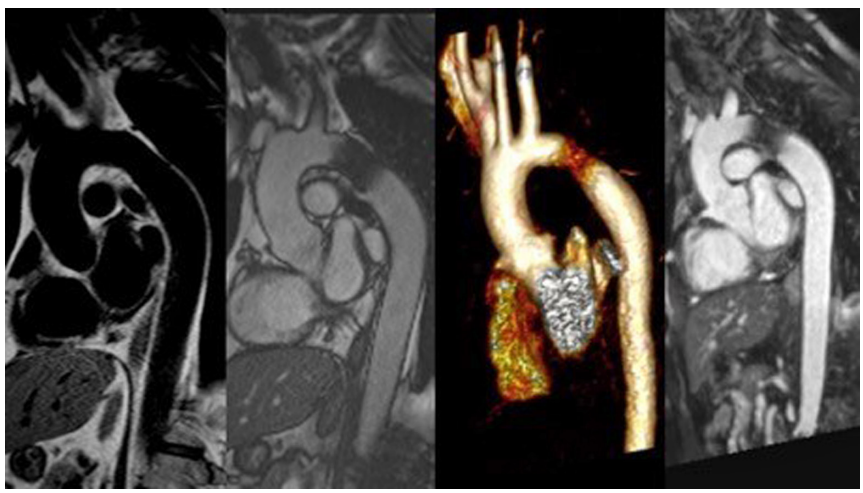

Figure 14
A case of coarctation of aorta following stent implantation. Different MRI techniques shown to investigate the intervened vascular structure. From left to right are black-blood, balanced SSFP cine, volume-rendered MR angiography and a multiplanar reconstruction from a 3-dimensional SSFP (3D whole heart) dataset.

https://erp.bioscientifica.com
https://doi.org/10.1530/ERP-19-0048

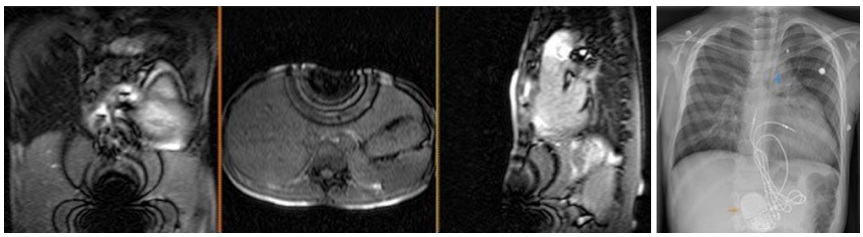

Figure 15
Artefacts from metal objects in MRI. This 11-year-old boy had MRI–conditional pacemaker and pacing leads (Medtronic SureScan) system and a left pulmonary artery stent *in situ*. Images 1, 2 and 3 represent the coronal, axial and sagittal views from the MRI survey. Image 4 is a chest X-ray of the same patient prior to MRI scan. The MRI-conditional pacemaker box (orange arrow) and left pulmonary artery stent (blue arrow) are shown.

region of interest, fetal and maternal motion. With the advent of novel image reconstruction techniques, it is now possible to obtain 3D whole heart imaging in the fetus (30) (Fig. 16) and assess flows throughout the fetal circulation (31). While much of this remains in a research arena, this a rapidly expanding area with some early clinical application already evident. Additional characterisation of extracardiac structures such as detection of pulmonary lymphangiectasia in the fetal lung which carries a poor prognosis in cases of hypoplastic left heart syndrome can also be very useful (32).

CMR-guided and augmented catheterisation

Comprehensive haemodynamic assessment requires invasive pressure measurements by means of cardiac catheterisation. It is possible to combine elements from a diagnostic cardiac catheterisation and a CMR study to provide more accurate haemodynamic assessment. An example of this is hybrid X-ray and MRI-guided catheterisation or catheterisation guided solely by MRI to not only produce accurate assessment of pulmonary vascular resistance but avoiding or reducing the need for radiation (33, 34). Assessment of pulmonary vascular resistance in this way is already considered a gold standard. MRI-guided catheterisation is a developing field with scope for MRI-guided cardiac interventions eliminating the need for radiation (35). Where an X-MR laboratory is not available patients may still be able to have CMR for flow and catheterisation for their pressures in order to facilitate more accurate pulmonary vascular resistance measurements thus using CMR to augment cardiac catheterisation.

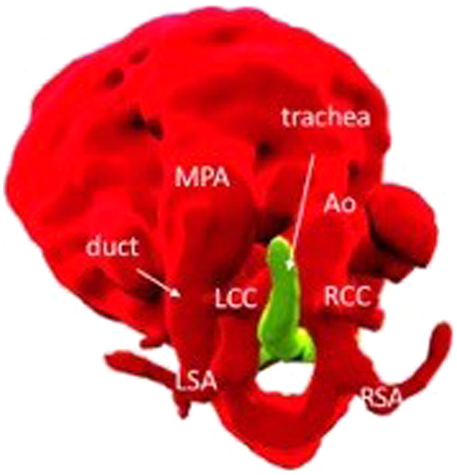

Figure 16
Volume-rendered view of a double aortic arch from a fetal CMR at 30 + 4 weeks gestation.

Cardiac CT

With the introduction of advanced CT scanners, cardiac CT has become an increasingly popular cross-sectional imaging platform due to its advantages of low-radiation dose exposure, easy access, short examination time and high image resolution (36). The short scanning time reduces the need for breath-holds and general anaesthesia. This is particularly favourable for clinically unstable patients who can only tolerate short examinations or un-cooperative patients who may be able to lie still for very short periods of time. Similar to CMR, CT provides comprehensive information of cardiac anatomy and surrounding vasculature in a three-dimensional view, with a higher level of detail. The latest generation of multidetector scanners are competitive, producing a spatial resolution of less than 0.5 mm (0.8–1.5 mm for MRI), and temporal resolution of less than 50 ms (37). Therefore, small structures such as coronary arteries and collateral vessels are well demonstrated using CT angiography over other imaging modalities. CHD patients require access to the most modern CT scanners as well as optimised protocols to enable them to have CT where indicated at significantly lower radiation dose (as discussed below).

In some cases, there are clear indications for CT rather than CMR. MR-conditional vascular stents, metal implants or surgical wires produce susceptibility artefacts (38) which may void the diagnostic value of the CMR study. These devices, however, are better tolerated using CT (Fig. 17A).

https://erp.bioscientifica.com
https://doi.org/10.1530/ERP-19-0048

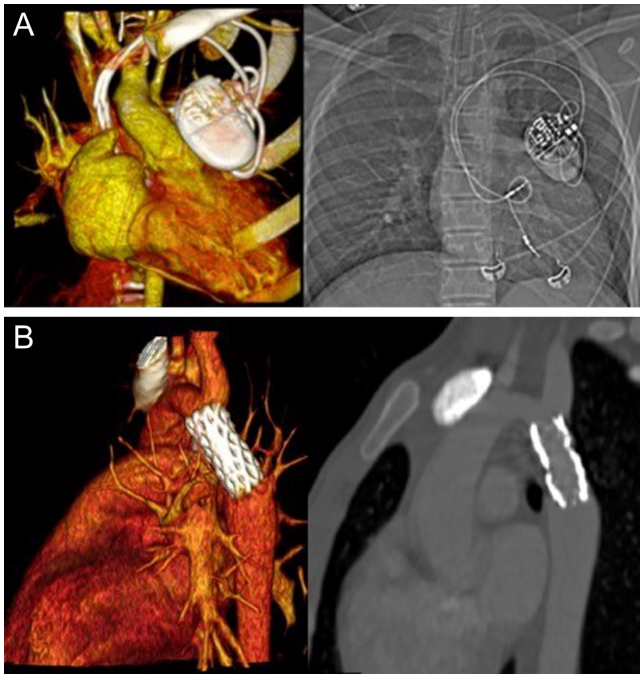

Figure 17
(A) Volume-rendered image of a pacemaker on a CT angiogram, paired with a plain CXR on the right. (B) Contrast-enhanced CT images showing volume rendered (left) and multiplanar reconstruction (MPR) (right) post coarctation stent.

CT is also more sensitive than CMR at detecting calcification (39) and vessel wall damage, infrequent but potentially serious complications associated with vascular grafts and stents (40). Hence, CT is often the preferred imaging modality in the immediate period following stent and device implantation (Fig. 17B) (41).

Radiation exposure in CT

CT collects imaging information by passing multiple X-ray beams through the body. However, X-ray exposure is not without risk as excessive exposure to X-ray results in irreparable damage to the tissue (42). The absorption limit varies between tissues types as rapidly growing structures are more vulnerable to radiation damage. Younger children with rapidly dividing cells are more affected by ionising radiation and therefore potentially worse affected, especially when the long-term effect is less well-studied compared to the adult population (42). Patients with CHD also require imaging surveillance and at risk from repeated exposure to radiation (43).

Due to such risks, CT is often reserved for specific questions that other imaging modalities cannot provide or contraindicated (such as having a non-MRI conditional pacemaker or being on mechanical support). This is particularly important as congenital heart disease patients need multiple scans for diagnostic and surveillance purposes throughout their life (44). Having recognised the potential lifelong risk associated with X-ray radiation exposure, modern CT scanners have incorporated radiation dose reduction technology, both by improvement in the overall design (for example, use of multidetector, faster gantry spinning speed of table movement and image reconstruction algorithms), as well as dose optimization protocol to minimize radiation exposure (45). Scanners can now acquire as many as 256–320 slices in one rotation, which coupled with increased speed allows the acquisition of thinner, higher spatial resolution slices whilst still covering the complete volume of the heart in one short breath-hold (46).

Such improvements have resulted in rapid acquisition times of less than one second per study, and images with high temporal resolution and overall radiation dose reduction compared to previous generations of scanners. For coronary CT angiogram, modern scanners produce radiation doses of <1 mSv, compared to 15–30 mSv in previous generations of machines or 3–6 mSv compared to invasive coronary angiography (47). The effective radiation dose for a low-dose coronary angiogram in children (48) is equivalent to 4–10 chest X-rays, or 1–3 months exposure to natural background radiation, once corrected for the normalised age and region-specific conversion factors derived from the International Commission on Radiological Protection publication 102 (49). In addition, at such high scanning speeds, the previous limitations of arrhythmia or heart rate control becomes tolerable (50). These advantages make it justifiable for the use of CT in younger patients, especially if high-risk general anaesthesia for cross-sectional imaging is required.

CT image acquisition

Current state-of-the-art CT scanners are composed of an X-ray tube, or tubes that are built into a rapidly spinning gantry. Within the gantry, the multiple arrays of detectors are constructed to the opposite side. The X-ray tube(s) emits radiation energy that can be modified, by altering the current strength (mAs) or the voltage (kV). The higher number of detectors can be fitted within the gantry, and the rotation speed of the tube rotation determines how much coverage can take place per rotation (51). Pitch indicates the relationship between the speed of gantry rotation, table movement and beam collimation. This allows overlapping between image acquisition volume per rotation. Using oversampling the reconstruction

https://erp.bioscientifica.com
https://doi.org/10.1530/ERP-19-0048

engine allows this form of low-pitch scanning to produce extremely high resolution of images (52).

ECG gating plays an important role of image quality as it minimizes the effect of cardiac motion. The scanner registers the position of the heart at a finite point of the cardiac cycle to acquire the images as prescribed. In retrospective ECG gating, images are acquired continuously throughout the cardiac cycle. This method produces the best quality images, as the operator can retrospectively reconstruct images with least motion artefacts at any time point during the cardiac cycle. This is particularly useful for small structures such as coronary arteries or segments of coronary arteries which are prone to motion artefacts. The drawback of this method is radiation dose exposure (53).

However, technological advances now allow for prospective acquisitions with good image quality while still achieving low radiation doses (54, 55). With prospective ECG triggering, images are obtained at the set time point or window (millisecond or percentage of the R-R interval), often during mid systole or mid diastole when the heart is assumed to have the least motion. Radiation dose is saved using this method; however, if selection period is incorrect, or unpredictable due to arrhythmias, the acquisition may have to be repeated.

Images can also be acquired without ECG gating. This will produce the most motion artefact, but radiation dose will be the least. Extra manoeuvres to eliminate motion includes breath-holding or the use of rate-modulating medication such as β-blockers or ivabradine (56).

Assessment of ventricular function

Using retrospective ECG gating CT, ventricular volumetric and functional assessment can be carried out (57). The drawback is high radiation dose exposure and therefore should be reserved for cases when there is no alternative or limited information from echocardiography or CMR.

Data interpretation and image processing tools

The quality and accuracy of the final reconstructed images can only be as good as the original dataset. Due to radiation reduction strategies, most cardiac CT acquisitions are not gated by ECG or only gated to a small fraction of the cardiac cycle. It is also dependent on the use of contrast agent (site of injection, the rate of infusion (relative to cardiac output)) and the presence of shunt in the cardiac lesions. The timing of acquisition based on all these above factors which can vary significantly and may not enhance the desired structures. Repeat acquisition in the delayed phase is rarely required and must be exercised with care, to minimise the radiation burden.

Similar to CMR and echocardiography, there are vendor-specific but also numerous freely licensed software that facilitate off-cart/offline post-processing of CT data. Common tools include cropping, 3D rendering and multiplanar reconstruction. All of which allow focused examination and presentation of the desired structures. Many Picture Archiving and Communication System (PACS) packages available in hospitals have these functions integrated, allowing rapid reconstruction and demonstration of vital information.

Practical considerations for CT scanning

Only recently, with the availability of 3rd generation CT scanners described above, neonatal cardiac CT has been considered acceptable for judicious use as an adjunct to echocardiography and MRI. Practice varies between local policies and resources determining the threshold for the use of cardiac CT in newborns. The main indication for cardiac CT in newborns is to define extra-cardiac vascular anatomy not achievable by conventional echocardiography due to limited acoustic windows or where diagnostic cardiac catheterisation is deemed too invasive.

CT scans in newborns can be performed using a 'feed and wrap' strategy where a baby who already has an intravenous cannula in place has a feed and is wrapped in blanket to reduce any effects of sudden movements. The baby falls into a natural sleep allowing the scan to be performed. In infants and older children, administration of sedative agents by oral, buccal or intranasal routes allows the scan to be performed. In very few cases, a general anaesthetic is required, particularly in patients with significant learning difficulties and behavioural challenges. Some patients may be critically ill and require a CT while intubated, and in some cases on mechanical support (ECMO).

Specific examples of cardiac CT in CHD

Complex vascular information is often needed as part of the diagnosis and planning in severe cardiac malformations (functionally single ventricle, or atresia of outlet valves), complex aortic arch obstruction, laterality disorder, anomalous pulmonary venous drainage (often mixed type), and determining pulmonary blood supply in pulmonary atresia. CT coronary angiography is used

https://erp.bioscientifica.com
https://doi.org/10.1530/ERP-19-0048

when there is uncertainty of coronary artery anatomy on echocardiography or CMR.

Aortic arch anatomy

Cardiac CT can provide accurate detail on arch anatomy, relationship of head and neck vessels, as well the site and extent of a narrowed segment to determine the management plan such as whether surgery is indicated, the timing of surgery, the extent of surgery (coarctation repair or extended arch reconstruction), and surgical approach (median sternotomy or lateral thoracotomy) (Fig. 18). However, it must be stressed that preoperative isolated aortic coarctation alone in the newborn is not a strong indication for CT, as most of the information can be gained through echocardiography and one should reserve the potential harmful effects of radiation for more complex lesions. In the post-surgical or interventional catheter intervention setting it can help identify the site and extent of recurrent or residual lesions.

Pulmonary artery anatomy

Pulmonary atresia VSD MAPCAS is a cyanotic heart condition, the native pulmonary arteries may be significantly hypoplastic or absent with additional blood supply to lung segments arising via major aorto-pulmonary collateral arteries (MAPCAs) from the aorta. Detailed information on the pulmonary blood supply is required for unifocalisation and reconstruction of the pulmonary arteries, which is often carried out in multiple stages (Fig. 19 and Video 6) The high spatial resolution of CT provides a distinct advantage over MRI and echocardiography to help define these vessels, and it is increasingly used early in the assessment of this condition. However, some lung segments have two sources of blood supply from both the native pulmonary artery and MAPCAs. This can only be assessed by means of selective injections into the individual MAPCAs during diagnostic cardiac catheterisation.

Video 6
Contrast-enhanced CT of pulmonary atresia, ventricular septal defect and MAPCA (major aortopulmonary collateral arteries) and right-sided aortic arch. The main pulmonary artery has been anastomosed with a classic central shunt created by the left subclavian artery. This patient has been unifocalised, with some residual MAPCAS. View Video 6 at http://movie-usa.glencoesoftware.com/video/10.1530/ERP-19-0048/video-6.

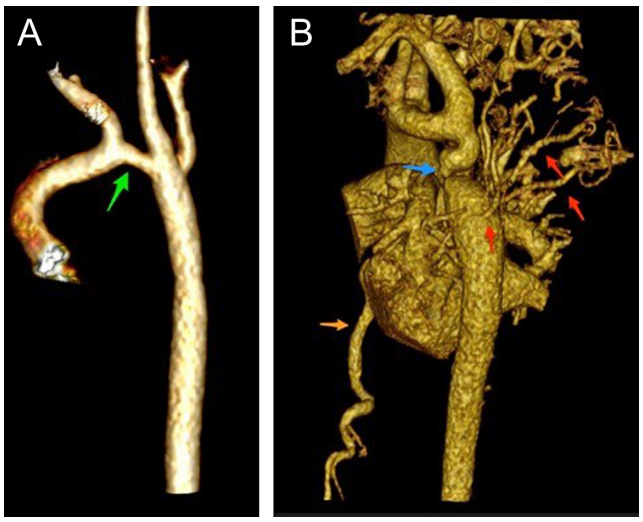

Figure 18
Volume-rendered images of aortic arch. Image (A) (to the left) was aortic arch of an infant following surgical repair, with residual transverse arch hypoplasia (green arrow). Image (B) (to the right) shows a case of coarctation in an older child (12 years). There is transverse arch hypoplasia, tortuous isthmus with coarctation (blue arrow). There is post-coarctation dilatation. Extensive network of thoracic collateral vessels (red arrows) and dilated intermammary arteries (orange arrow).

Figure 19
Contrast-enhanced CT of pulmonary atresia, ventricular septal defect and MAPCA (major aortopulmonary collateral arteries) and right-sided aortic arch. The main pulmonary artery has been anastomosed with a classic central shunt created by the left subclavian artery. This patient has been unifocalised, with some residual MAPCAS. The study was done to assess anatomy prior to RV-PA conduit reconstruction.

https://erp.bioscientifica.com
https://doi.org/10.1530/ERP-19-0048

Tetralogy of Fallot also requires detailed information on the morphology and calibre of the main pulmonary artery and branches and coronary artery anatomy. The key information to exclude is the proximity and course of the left mainstem/left anterior descending artery in relation to the RV outflow tract (RVOT) in the planning for percutaneous pulmonary valve implantation or surgery to avoid coronary artery compression following stent deployment. This can mainly be achieved with CMR which also evaluates of pulmonary regurgitation, right ventricular volumes and degree of aortopathy. CT is helpful in the assessment of calcification in RVOT which can relate to a risk of rupture for percutaneous pulmonary valve implantation (58).

Arterial shunts and ductal stents

Echocardiography provides essential function about ventricular function, volume and valvular regurgitation in most patients. Branch pulmonary artery and shunt flow (modified BT shunt or Sano shunt) can be screened using echocardiography but does not provide sufficient detail. Low radiation cardiac CT is can be used routinely to ensure shunt patency, adequate branch PA growth and their proximity to the superior vena cava (Fig. 20) prior to Norwood stage II operation (superior cavopulmonary anastomosis) or in the event of a clinical decompensation instead of invasive catheterisation.

Coronary artery anatomy

Anomalous coronary artery from the pulmonary artery (ALCAPA) is a rare congenital heart disease when the left coronary artery arises from the main pulmonary trunk rather than the aortic root. The origin of the anomalous left coronary, with flow reversal on colour Doppler are adequate to make a diagnosis of ALCAPA. However, in some instances, CT coronary angiogram is helpful in supporting the echocardiographic findings (Fig. 21). Prior to surgery, functional assessment and tissue characterisation by CMR is of less clinical relevance as such poorly functioning heart is known to recover following reimplantation of the left coronary artery.

An abnormal coronary course is also found in other forms of CHD such as transposition of great arteries and can pose difficulties with the technical aspects of surgery. Echocardiography is an excellent tool to demonstrate this, and CT is only used where there is diagnostic uncertainty from echocardiography.

Figure 20
Contrast-enhanced rendered volume of a patent with hypoplastic left heart syndrome following Norwood stage I with right modified BT shunt. The shunt (B) is patent and anastomosed to the right pulmonary artery (R). The left pulmonary artery (L) is slender. The reconstructed aortic arch (A) and Damus Kaye Stansel (D) anastomosis is patent.

Total anomalous pulmonary venous drainage

The majority of patients do not need cardiac CT or MRI; however, in some children where there is suspicion of mixed type TAPVD, or suboptimal echocardiographic windows, such investigations would become helpful. Both CMR and CT can equally provide good quality of anatomical information, as well as identify reasons for obstruction or potential for obstruction.

Complex biventricular repair/septation

Some forms of CHD present with challenges in decision making as to the suitability for biventricular repair. Examples include unbalanced AVSD and some forms of double outlet right ventricle. In addition to 2D and 3D echocardiography, CT and CMR play a substantial role in determining the cardiac connections, coronary artery anatomy and AV valve relationships. 3D information is essential in the surgical planning.

Airways assessment

The airways can be compressed by vascular structures such as a vascular ring (e.g. Double aortic arch). Cardiac CT combined with dynamic breath-hold manoeuvres could reveal important functional information of the airways. When combined with an endoscopic bronchoscopy, this is a very useful diagnostic test.

3D printing

3D printing is increasingly used to successfully plan surgical or catheter-based interventions in CHD as it

https://erp.bioscientifica.com
https://doi.org/10.1530/ERP-19-0048

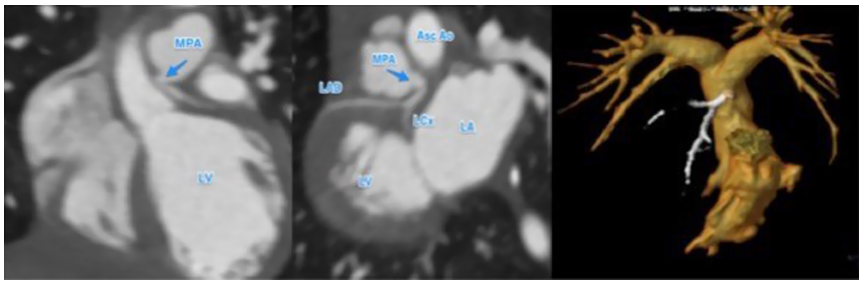

Figure 21
Anomalous left coronary artery arising from the main pulmonary artery (MPA). The left coronary artery does not arise from the aortic root (left hand image). The left coronary ostium is traced back to the MPA. This gives rise to the left anterior descending artery (LAD) and left circumflex (LCx). The left ventricle (LV) and left atrium (LA) are dilated, in association with impaired ventricular function prior to surgery. The right-hand image shows a volume rendered view of the right ventricle, MPA and branch pulmonary arteries (yellow). The left coronary artery (white) arise for the MPA.

allows the team to not only handle the object but to simulate the intervention in advance of the procedure. 3D whole heart imaging derived either from CT or MRI can be used to generate segmented images which are then saved as stereolithography (STL) files. These are then sent to a computer aided design software where further refinement of the image is performed to create hollow models with smooth surfaces, which can be reviewed as a 3D PDF file or printed into a model. This summarised in a recent review on 3D printing in CHD by Velasco-Forte *et al.* (59). Augmented or virtual reality is also increasingly being used as a means to project and interact with CMR and CT data.

Conclusion

We have given an overview of CMR and CT approaches including examples of their application to congenital heart disease. In future, it is likely that does reduction for CT will further improve and resolution increase. CMR will become faster. Its application in congenital heart disease requires specific expertise and skill, studies can be lengthy compared to echocardiography which is also more available and post processing can be laborious. With time, CMR will become faster, move further towards operator-independent acquisitions and post processing will become more automated even for congenital heart disease. Meanwhile, CMR and CT for children and adults with congenital heart disease is best performed in centres with a high volume of practice and dedicated congenital heart disease expertise.

Declaration of interest
The authors declare that there is no conflict of interest that could be perceived as prejudicing the impartiality of this review.

Funding
Dr Phuoc Duong is supported by the National Institute for Health Research (NIHR) Cardiovascular MedTech Co-operative. The views expressed are those of the authors and not necessarily those of the NIHR or the Department of Health and Social Care. Dr Sonya Babu-Narayan is supported by the British Heart Foundation (FS/11/38/28864).

References

1 Valente AM, Cook S, Festa P, Ko HH, Krishnamurthy R, Taylor AM, Warnes CA, Kreutzer J & Geva T. Multimodality imaging guidelines for patients with repaired tetralogy of Fallot: a report from the American Society of Echocardiography: developed in collaboration with the Society for Cardiovascular Magnetic Resonance and the Society for Pediatric Radiology. *Journal of the American Society of Echocardiography* 2014 **27** 111–141. (https://doi.org/10.1016/j.echo.2013.11.009)
2 Cohen MS, Eidem BW, Cetta F, Fogel MA, Frommelt PC, Ganame J, Han BK, Kimball TR, Johnson RK, Mertens L, *et al.* Multimodality imaging guidelines of patients with transposition of the great arteries: a report from the American Society of Echocardiography developed in collaboration with the Society for Cardiovascular Magnetic Resonance and the Society of Cardiovascular Computed Tomography. *Journal of the American Society of Echocardiography* 2016 **29** 571–621. (https://doi.org/10.1016/j.echo.2016.04.002)
3 Di Salvo G, Miller O, Babu Narayan S, Li W, Budts W, Valsangiacomo Buechel ER, Frigiola A, van den Bosch AE, Bonello B, Mertens L, *et al.* Imaging the adult with congenital heart disease: a multimodality imaging approach-position paper from the EACVI. *European Heart Journal: Cardiovascular Imaging* 2018 **19** 1077–1098. (https://doi.org/10.1093/ehjci/jey102)
4 D'Alto M, Dimopoulos K, Budts W, Diller GP, Di Salvo G, Dellegrottaglie S, Festa P, Scognamiglio G, Rea G, Ait Ali L, *et al.* Multimodality imaging in congenital heart disease-related pulmonary arterial hypertension. *Heart* 2016 **102** 910–918. (https://doi.org/10.1136/heartjnl-2015-308903)
5 Luijnenburg SE, Robbers-Visser D, Moelker A, Vliegen HW, Mulder BJ & Helbing WA. Intra-observer and interobserver variability of biventricular function, volumes and mass in patients with congenital heart disease measured by CMR imaging. *International Journal of Cardiovascular Imaging* 2010 **26** 57–64. (https://doi.org/10.1007/s10554-009-9501-y)
6 Fratz S, Chung T, Greil GF, Samyn MM, Taylor AM, Valsangiacomo Buechel ER, Yoo SJ & Powell AJ. Guidelines and protocols for cardiovascular magnetic resonance in children and adults with congenital heart disease: SCMR expert consensus group on congenital heart disease. *Journal of Cardiovascular Magnetic Resonance* 2013 **15** 51. (https://doi.org/10.1186/1532-429X-15-51)
7 Valsangiacomo Buechel ER, Grosse-Wortmann L, Fratz S, Eichhorn J, Sarikouch S, Greil GF, Beerbaum P, Bucciarelli-Ducci C, Bonello B, Sieverding L, *et al.* Indications for cardiovascular magnetic resonance in children with congenital and acquired heart disease: an expert consensus paper of the Imaging Working Group of the AEPC and the Cardiovascular Magnetic Resonance Section of the EACVI. *European Heart Journal: Cardiovascular Imaging* 2015 **16** 281–297. (https://doi.org/10.1093/ehjci/jeu129)

8 Bonnemains L, Raimondi F & Odille F. Specifics of cardiac magnetic resonance imaging in children. *Archives of Cardiovascular Diseases* 2016 **109** 143–149. (https://doi.org/10.1016/j.acvd.2015.11.004)

9 Vassiliou VS, Cameron D, Prasad SK & Gatehouse PD. Magnetic resonance imaging: physics basics for the cardiologist. *JRSM Cardiovascular Disease* 2018 **7** 2048004018772237. (https://doi.org/10.1177/2048004018772237)

10 Schievano S, Capelli C, Young C, Lurz P, Nordmeyer J, Owens C, Bonhoeffer P & Taylor AM. Four-dimensional computed tomography: a method of assessing right ventricular outflow tract and pulmonary artery deformations throughout the cardiac cycle. *European Radiology* 2011 **21** 36–45. (https://doi.org/10.1007/s00330-010-1913-5)

11 Winter MM, Bernink FJ, Groenink M, Bouma BJ, van Dijk AP, Helbing WA, Tijssen JG & Mulder BJ. Evaluating the systemic right ventricle by CMR: the importance of consistent and reproducible delineation of the cavity. *Journal of Cardiovascular Magnetic Resonance* 2008 **10** 40. (https://doi.org/10.1186/1532-429X-10-40)

12 Dardeer AM, Hudsmith L, Wesolowski R, Clift P & Steeds RP. The potential role of feature tracking in adult congenital heart disease: advantages and disadvantages in measuring myocardial deformation by cardiovascular magnetic resonance. *Journal of Congenital Cardiology* 2018 **2** 3. (https://doi.org/10.1186/s40949-018-0015-0)

13 Orwat S, Diller GP, Kempny A, Radke R, Peters B, Kuhne T, Boethig D, Gutberlet M, Dubowy KO, Beerbaum P, *et al*. Myocardial deformation parameters predict outcome in patients with repaired tetralogy of Fallot. *Heart* 2016 **102** 209–215. (https://doi.org/10.1136/heartjnl-2015-308569)

14 Moon TJ, Choueiter N, Geva T, Valente AM, Gauvreau K & Harrild DM. Relation of biventricular strain and dyssynchrony in repaired tetralogy of Fallot measured by cardiac magnetic resonance to death and sustained ventricular tachycardia. *American Journal of Cardiology* 2015 **115** 676–680. (https://doi.org/10.1016/j.amjcard.2014.12.024)

15 Beerbaum P, Korperich H, Barth P, Esdorn H, Gieseke J & Meyer H. Noninvasive quantification of left-to-right shunt in pediatric patients: phase-contrast cine magnetic resonance imaging compared with invasive oximetry. *Circulation* 2001 **103** 2476–2482. (https://doi.org/10.1161/01.cir.103.20.2476)

16 Grosse-Wortmann L, Al-Otay A & Yoo SJ. Aortopulmonary collaterals after bidirectional cavopulmonary connection or Fontan completion: quantification with MRI. *Circulation: Cardiovascular Imaging* 2009 **2** 219–225. (https://doi.org/10.1161/CIRCIMAGING.108.834192)

17 Whitehead KK, Gillespie MJ, Harris MA, Fogel MA & Rome JJ. Noninvasive quantification of systemic-to-pulmonary collateral flow: a major source of inefficiency in patients with superior cavopulmonary connections. *Circulation: Cardiovascular Imaging* 2009 **2** 405–411. (https://doi.org/10.1161/CIRCIMAGING.108.832113)

18 Dyverfeldt P, Bissell M, Barker AJ, Bolger AF, Carlhäll CJ, Ebbers T, Francios CJ, Frydrychowicz A, Geiger J, Giese D, *et al*. 4D flow cardiovascular magnetic resonance consensus statement. *Journal of Cardiovascular Magnetic Resonance* 2015 **17** 72. (https://doi.org/10.1186/s12968-015-0174-5)

19 Rathod RH, Powell AJ & Geva T. Myocardial fibrosis in congenital heart disease. *Circulation Journal* 2016 **80** 1300–1307. (https://doi.org/10.1253/circj.CJ-16-0353)

20 Babu-Narayan SV, Goktekin O, Moon JC, Broberg CS, Pantely GA, Pennell DJ, Gatzoulis MA & Kilner PJ. Late gadolinium enhancement cardiovascular magnetic resonance of the systemic right ventricle in adults with previous atrial redirection surgery for transposition of the great arteries. *Circulation* 2005 **111** 2091–2098. (https://doi.org/10.1161/01.CIR.0000162463.61626.3B)

21 Babu-Narayan SV, Kilner PJ, Li W, Moon JC, Goktekin O, Davlouros PA, Khan M, Ho SY, Pennell DJ & Gatzoulis MA. Ventricular fibrosis suggested by cardiovascular magnetic resonance in adults with repaired tetralogy of Fallot and its relationship to adverse markers of clinical outcome. *Circulation* 2006 **113** 405–413. (https://doi.org/10.1161/CIRCULATIONAHA.105.548727)

22 Rydman R, Gatzoulis MA, Ho SY, Ernst S, Swan L, Li W, Wong T, Sheppard M, McCarthy KP, Roughton M, *et al*. Systemic right ventricular fibrosis detected by cardiovascular magnetic resonance is associated with clinical outcome, mainly new-onset atrial arrhythmia, in patients after atrial redirection surgery for transposition of the great arteries. *Circulation: Cardiovascular Imaging* 2015 **8** e002628. (https://doi.org/10.1161/CIRCIMAGING.114.002628)

23 Rathod RH, Prakash A, Powell AJ & Geva T. Myocardial fibrosis identified by cardiac magnetic resonance late gadolinium enhancement is associated with adverse ventricular mechanics and ventricular tachycardia late after Fontan operation. *Journal of the American College of Cardiology* 2010 **55** 1721–1728. (https://doi.org/10.1016/j.jacc.2009.12.036)

24 Gagliardi MG, Bevilacqua M, Di Renzi P, Picardo S, Passariello R & Marcelletti C. Usefulness of magnetic resonance imaging for diagnosis of acute myocarditis in infants and children, and comparison with endomyocardial biopsy. *American Journal of Cardiology* 1991 **68** 1089–1091. (https://doi.org/10.1016/0002-9149(91)90501-b)

25 Raimondi F, Iserin F, Raisky O, Laux D, Bajolle F, Boudjemline Y, Boddaert N & Bonnet D. Myocardial inflammation on cardiovascular magnetic resonance predicts left ventricular function recovery in children with recent dilated cardiomyopathy. *European Heart Journal: Cardiovascular Imaging* 2015 **16** 756–762. (https://doi.org/10.1093/ehjci/jev002)

26 Banka P, Robinson JD, Uppu SC, Harris MA, Hasbani K, Lai WW, Richmond ME, Fratz S, Jain S, Johnson TR, *et al*. Cardiovascular magnetic resonance techniques and findings in children with myocarditis: a multicenter retrospective study. *Journal of Cardiovascular Magnetic Resonance* 2015 **17** 96. (https://doi.org/10.1186/s12968-015-0201-6)

27 Beroukhim RS, Prakash A, Valsangiacomo Buechel ER, Cava JR, Dorfman AL, Festa P, Hlavacek AM, Johnson TR, Keller MS, Krishnamurthy R, *et al*. Characterization of cardiac tumors in children by cardiovascular magnetic resonance imaging: a multicenter experience. *Journal of the American College of Cardiology* 2011 **58** 1044–1054. (https://doi.org/10.1016/j.jacc.2011.05.027)

28 Raimondi F, Aquaro GD, De Marchi D, Sandrini C, Khraiche D, Festa P, Ait Ali L, Boddaert N & Bonnet D. Cardiac magnetic resonance myocardial perfusion after arterial switch for transposition of great arteries. *JACC: Cardiovascular Imaging* 2018 **11** 778–779. (https://doi.org/10.1016/j.jcmg.2017.07.015)

29 Muthalaly RG, Nerlekar N, Ge Y, Kwong RY & Nasis A. MRI in patients with cardiac implantable electronic devices. *Radiology* 2018 **289** 281–292. (https://doi.org/10.1148/radiol.2018180285)

30 Lloyd DFA, Pushparajah K, Simpson JM, van Amerom JFP, van Poppel MPM, Schulz A, Kainz B, Deprez M, Lohezic M, Allsop J, *et al*. Three-dimensional visualisation of the fetal heart using prenatal MRI with motion-corrected slice-volume registration: a prospective, single-centre cohort study. *Lancet* 2019 **393** 1619–1627. (https://doi.org/10.1016/S0140-6736(18)32490-5)

31 Seed M, van Amerom JF, Yoo SJ, Al Nafisi B, Grosse-Wortmann L, Jaeggi E, Jansz MS & Macgowan CK. Feasibility of quantification of the distribution of blood flow in the normal human fetal circulation using CMR: a cross-sectional study. *Journal of Cardiovascular Magnetic Resonance* 2012 **14** 79. (https://doi.org/10.1186/1532-429X-14-79)

32 Saul D, Degenhardt K, Iyoob SD, Surrey LF, Johnson AM, Johnson MP, Rychik J & Victoria T. Hypoplastic left heart syndrome and the nutmeg lung pattern in utero: a cause and effect relationship or prognostic indicator? *Pediatric Radiology* 2016 **46** 483–489. (https://doi.org/10.1007/s00247-015-3514-6)

33 Razavi R, Hill DL, Keevil SF, Miquel ME, Muthurangu V, Hegde S, Rhode K, Barnett M, van Vaals J, Hawkes DJ, *et al*. Cardiac

catheterisation guided by MRI in children and adults with congenital heart disease. *Lancet* 2003 **362** 1877–1882. (https://doi.org/10.1016/S0140-6736(03)14956-2)
34 Muthurangu V, Taylor A, Andriantsimiavona R, Hegde S, Miquel ME, Tulloh R, Baker E, Hill DL & Razavi RS. Novel method of quantifying pulmonary vascular resistance by use of simultaneous invasive pressure monitoring and phase-contrast magnetic resonance flow. *Circulation* 2004 **110** 826–834. (https://doi.org/10.1161/01.CIR.0000138741.72946.84)
35 Pushparajah K, Chubb H & Razavi R. MR-guided cardiac interventions. *Topics in Magnetic Resonance Imaging* 2018 **27** 115–128. (https://doi.org/10.1097/RMR.0000000000000156)
36 Crean A. Cardiovascular MR and CT in congenital heart disease. *Heart* 2007 **93** 1637–1647. (https://doi.org/10.1136/hrt.2006.104729)
37 National Institute for Health and Care Excellence. New generation cardiac CT scanners (Aquilion ONE, Brilliance iCT, Discovery CT750 HD and Somatom Definition Flash) for cardiac imaging in people with suspected or known coronary artery disease in whom imaging is difficult with earlier generation CT scanners. London, UK: NICE, 2017. (available at: https://www.nice.org.uk/guidance/dg3/resources)
38 Stadler A, Schima W, Ba-Ssalamah A, Kettenbach J & Eisenhuber E. Artifacts in body MR imaging: their appearance and how to eliminate them. *European Radiology* 2007 **17** 1242–1255. (https://doi.org/10.1007/s00330-006-0470-4)
39 Solie CJ, Mohr NM & Runde DP. Can multidetector computed tomography rule out left atrial thrombus in patients with atrial fibrillation? *Annals of Emergency Medicine* 2018 **71** 480–481. (https://doi.org/10.1016/j.annemergmed.2017.09.012)
40 Korperich H, Muller K, Barth P, Gieseke J, Haas N, Schulze-Neick I, Burchert W, Kececioglu D & Laser KT. Differentiation of impaired from preserved hemodynamics in patients with fontan circulation using real-time phase-velocity cardiovascular magnetic resonance. *Journal of Thoracic Imaging* 2017 **32** 159–168. (https://doi.org/10.1097/RTI.0000000000000261)
41 Blum MB, Schmook M, Schernthaner R, Edelhauser G, Puchner S, Lammer J & Funovics MA. Quantification and detectability of in-stent stenosis with CT angiography and MR angiography in arterial stents in vitro. *American Journal of Roentgenology* 2007 **189** 1238–1242. (https://doi.org/10.2214/AJR.07.2501)
42 Gherardi GG, Iball GR, Darby MJ & Thomson JD. Cardiac computed tomography and conventional angiography in the diagnosis of congenital cardiac disease in children: recent trends and radiation doses. *Cardiology in the Young* 2011 **21** 616–622. (https://doi.org/10.1017/S1047951111000485)
43 Hoffmann A, Engelfriet P & Mulder B. Radiation exposure during follow-up of adults with congenital heart disease. *International Journal of Cardiology* 2007 **118** 151–153. (https://doi.org/10.1016/j.ijcard.2006.07.012)
44 Orwat S, Diller GP & Baumgartner H. Imaging of congenital heart disease in adults: choice of modalities. *European Heart Journal Cardiovascular Imaging* 2014 **15** 6–17. (https://doi.org/10.1093/ehjci/jet124)
45 Goldman LW. Principles of CT and CT technology. *Journal of Nuclear Medicine Technology* 2007 **35** 115–128; quiz 129–130. (https://doi.org/10.2967/jnmt.107.042978)
46 Hsiao EM, Rybicki FJ & Steigner M. CT coronary angiography: 256-slice and 320-detector row scanners. *Current Cardiology Reports* 2010 **12** 68–75. (https://doi.org/10.1007/s11886-009-0075-z)
47 Nie P, Wang X, Cheng Z, Ji X, Duan Y & Chen J. Accuracy, image quality and radiation dose comparison of high-pitch spiral and sequential acquisition on 128-slice dual-source CT angiography in children with congenital heart disease. *European Radiology* 2012 **22** 2057–2066. (https://doi.org/10.1007/s00330-012-2479-1)
48 Duan Y, Wang X, Cheng Z, Wu D & Wu L. Application of prospective ECG-triggered dual-source CT coronary angiography for infants and children with coronary artery aneurysms due to Kawasaki disease. *British Journal of Radiology* 2012 **85** e1190–e1197. (https://doi.org/10.1259/bjr/18174517)
49 Valentin J & International Commission on Radiation Protection. Managing patient dose in multi-detector computed tomography(MDCT). ICRP Publication 102. *Annals of the ICRP* 2007 **37** 1–79, iii.
50 Chao SP, Leu JG, Law WY, Kuo CJ & Shyu KG. Image quality of 256-slice computed tomography for coronary angiography. *Acta Cardiologica Sinica* 2013 **29** 444–450.
51 Silverman PM, Kalender WA & Hazle JD. Common terminology for single and multislice helical CT. *American Journal of Roentgenology* 2001 **176** 1135–1136. (https://doi.org/10.2214/ajr.176.5.1761135)
52 Ranallo FN & Szczykutowicz T. The correct selection of pitch for optimal CT scanning: avoiding common misconceptions. *Journal of the American College of Radiology* 2015 **12** 423–424. (https://doi.org/10.1016/j.jacr.2014.12.017)
53 Podberesky DJ, Angel E, Yoshizumi TT, Toncheva G, Salisbury SR, Alsip C, Barelli A, Egelhoff JC, Anderson-Evans C, Nguyen GB, *et al.* Radiation dose estimation for prospective and retrospective ECG-gated cardiac CT angiography in infants and small children using a 320-MDCT volume scanner. *American Journal of Roentgenology* 2012 **199** 1129–1135. (https://doi.org/10.2214/AJR.12.8480)
54 Habib Geryes B, Calmon R, Donciu V, Khraiche D, Warin-Fresse K, Bonnet D, Boddaert N & Raimondi F. Low-dose paediatric cardiac and thoracic computed tomography with prospective triggering: is it possible at any heart rate? *Physica Medica* 2018 **49** 99–104. (https://doi.org/10.1016/j.ejmp.2018.05.015)
55 Habib Geryes B, Calmon R, Khraiche D, Boddaert N, Bonnet D & Raimondi F. Radiation dose reduction in paediatric coronary computed tomography: assessment of effective dose and image quality. *European Radiology* 2016 **26** 2030–2038. (https://doi.org/10.1007/s00330-015-4032-5)
56 Pannu HK, Alvarez Jr W & Fishman EK. Beta-blockers for cardiac CT: a primer for the radiologist. *American Journal of Roentgenology* 2006 **186** S341–S345. (https://doi.org/10.2214/AJR.04.1944)
57 Rizvi A, Deano RC, Bachman DP, Xiong G, Min JK & Truong QA. Analysis of ventricular function by CT. *Journal of Cardiovascular Computed Tomography* 2015 **9** 1–12. (https://doi.org/10.1016/j.jcct.2014.11.007)
58 Boudjemline Y, Malekzadeh-Milani S, Patel M, Thambo JB, Bonnet D, Iserin L & Fraisse A. Predictors and outcomes of right ventricular outflow tract conduit rupture during percutaneous pulmonary valve implantation: a multicentre study. *EuroIntervention* 2016 **11** 1053–1062. (https://doi.org/10.4244/EIJY14M09_06)
59 Forte MNV, Hussain T, Roest A, Gomez G, Jongbloed M, Simpson J, Pushparajah K, Byrne N & Valverde I. Living the heart in three dimensions: applications of 3D printing in CHD. *Cardiology in the Young* 2019 **29** 733–743. (https://doi.org/10.1017/S1047951119000398)

Received in final form 3 September 2019
Accepted 15 October 2019
Accepted Manuscript published online 15 October 2019